

Validating Ellipsoid Zone Area Measurement With Multimodal Imaging in Choroideremia

Yi Zhai¹, Sarah Oke¹, and Ian M. MacDonald¹

¹ Department of Ophthalmology and Visual Sciences, University of Alberta, Edmonton, Alberta, Canada

Correspondence: Ian M. MacDonald, University of Alberta, 7-030 Katz Group Centre, Edmonton, Alberta T6G 2E1, Canada.
e-mail: macdonal@ualberta.ca

Received: September 25, 2020

Accepted: March 9, 2021

Published: May 12, 2021

Keywords: choroideremia; OCT; ellipsoid zone; fundus autofluorescence; gene therapy

Citation: Zhai Y, Oke S, MacDonald IM. Validating ellipsoid zone area measurement with multimodal imaging in choroideremia. *Transl Vis Sci Technol.* 2021;10(6):17, <https://doi.org/10.1167/tvst.10.6.17>

Purpose: To assess en face ellipsoid zone (EZ) maps of remaining retinal structure as outcome measures for the future clinical research in patients with choroideremia.

Methods: Twenty eyes from 12 patients with a confirmed genetic diagnosis of choroideremia were included retrospectively from a single site. From spectral domain-optical coherence tomography volume scans, slabs including the EZ were manually segmented to create the en face EZ maps. The preserved EZ area was measured by two graders. Lengths of the EZ were recorded at 0°, 45°, 90°, and 135°. The intraclass correlation coefficients and Bland–Altman plots were used to show intergrader agreement. The Pearson correlation coefficient evaluated the correlation between length and area. A Bland–Altman plot compared en face EZ and the preserved fundus autofluorescence area.

Results: Measurements of EZ area by two graders showed excellent agreement with an intraclass correlation coefficient of 0.992 (95% confidence interval, 0.980–0.997). A Pearson correlation analysis showed that the existing marker for preserved photoreceptor (horizontal EZ length) was correlated with the area ($r = 0.722$). The average EZ length in four meridians showed a much better correlation with the EZ area ($r = 0.929$). The fundus autofluorescence area was found to be a mean of $0.45 \pm 0.99 \text{ mm}^2$ greater than the EZ area.

Conclusions: EZ area measurement provides excellent intergrader reliability, although the process is time consuming. We propose a less time-consuming alternative to estimate the EZ by using the average EZ band length in meridians. Our data also suggest that the loss of photoreceptor inner segments is an early change in choroideremia and may happen before the loss of the retinal pigment epithelium.

Translational Relevance: En face EZ mapping is a potential tool for future clinical trials to quantify preserved photoreceptor structure in choroideremia.

Introduction

Choroideremia (CHM; OMIM #303100) is an X-linked retinal dystrophy that leads to the degeneration of the choriocapillaris, the retinal pigment epithelium, and the photoreceptors of the eye.¹ It is caused by loss-of-function mutations in the *CHM* gene and presumably amenable to CHM gene replacement therapy.²

Given its small size, the *CHM* gene (1.9 kb) can be easily accommodated within an adeno-associated virus 2 vector and delivered to the photoreceptors and retinal pigment epithelium by subretinal injection.³ During the past decade, several groups have reported

the outcomes of clinical trials of CHM with adeno-associated virus 2 using a variety of measures.^{3–6} Investigators seek accurate outcome measures to evaluate the effect of gene therapy on the outer retinal structures in patients with CHM, in particular the photoreceptors and retinal pigment epithelium. Among different imaging models, spectral domain-optical coherence tomography (SD-OCT) is considered to be a powerful tool to visualize the outer retinal structures.⁷

Some natural history studies have used either SD-OCT–derived central foveal thickness, subfoveal choroidal thickness, or preserved choriocapillaris to monitor the progression of CHM disease.^{8–10} The second hyper-reflective band of the retinal OCT,

termed the ellipsoid zone (EZ), has been associated with the photoreceptor inner segment ellipsoid.¹¹ The preserved horizontal EZ length has been used to estimate the remaining photoreceptors in inherited retinal dystrophies such as retinitis pigmentosa.¹² In a previous adeno-associated virus 2-mediated CHM gene therapy trial, our site used the EZ length across the macula as an estimate of preserved photoreceptor structure.⁴ However, the retinal atrophy in CHM typically has a scalloped margin with irregular retinal islands.¹³ A measurement of the preserved en face EZ area would be ideal and could provide a more accurate estimate of the preserved photoreceptors. An accurate measure of preserved en face EZ area has the potential to be used as a marker to monitor disease progression as well as to evaluate the efficacy of experimental therapies. In this study, we used SD-OCT volume scans from patients with CHM to create en face EZ maps. We explore the options for quantifying photoreceptor structure and provide outcome measurements for future clinical trials. We also evaluate the relationship between the EZ and the preserved fundus autofluorescence (FAF) area.

Methods

Description of the Study Subjects

The protocol of this study adhered to the tenets of the Declaration of Helsinki and was approved by the University of Alberta human research ethics board. We retrospectively reviewed all the available retinal images from patients with CHM in the Eye Institute of Alberta imaging databases.

The inclusion criteria for the study eye were as follows: (1) a confirmed genetic diagnosis of CHM. (2) the study eye had a 97-line raster OCT volume scan (Heidelberg Engineering, Heidelberg, Germany)

centered on the fovea, (3) the preserved retinal island fell within the OCT scanning window, and (4) the study eye had FAF imaging at the same visit.

Generation of the En Face EZ Map

All the OCT scans used to create en face EZ maps in this study consisted of 97 horizontal B-scans which covered the central $20^\circ \times 20^\circ$ area of the retina. The OCT volume scans included in this study used either a high-speed or a high-resolution mode. Inspired by the methods used by Hariri et al in their retinitis pigmentosa project,¹⁴ we aimed to further develop their method by manual segmentation of both outer and inner boundaries of the EZ. In order to create the en face EZ map, the distance between two B-scans must be less than $60 \mu\text{m}$. Using Bruch's membrane and the retinal pigment epithelium (RPE) as references, grader 1 (S.O.) manually segmented the outer and inner boundary of the EZ slabs (Fig. 1). For the area that entirely lacked EZ, a small slab of the outer nuclear layer was included to achieve a greater contrast between the preserved EZ and the background. For most cases, the outer boundary was placed at the gap between two hyper-reflective outer retinal bands (the EZ and the RPE/Bruch's membrane complex). For a few cases with burred boundaries between the EZ and the RPE/Bruch's membrane, the outer contour of the RPE/Bruch's membrane complex was used as a reference. The outer boundary line was displaced to $5 \mu\text{m}$ above the reference line. The inner boundary was placed right below the external limiting membrane if it was present or placed manually to include a part of the outer nuclear layer. The outer and inner boundaries were marked as PR1 and PR2 in the Heidelberg Eye Explorer 2 software (HEYEX 2, version 1.10.0.0). Grader 2 (Y.Z.) verified the segmentation generated by grader 1 and adjusted the segmentation

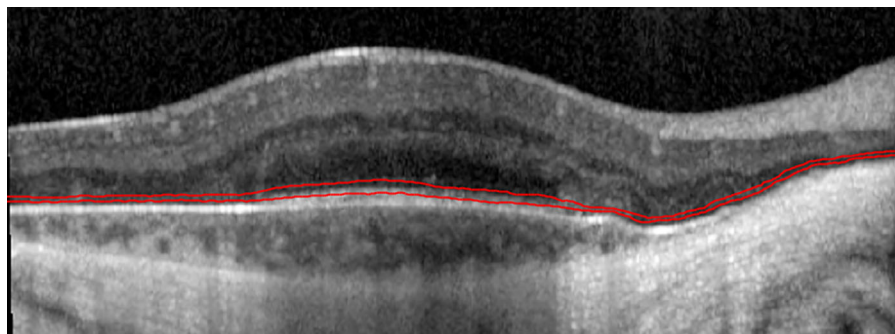


Figure 1. Segmentation of EZ element from an OCT scan. For the area that entirely lacked EZ, a small slab of the outer nuclear layer was included to achieve a greater contrast between preserved EZ and the background.

line to ensure EZ elements were precisely included in each B-scan. Using the three-dimensional transverse view function of HEYEX2, the en face EZ maps were generated with the maximum intensity projection.

Measurement of EZ Area and EZ Length

Using the “draw region” function in HEYEX2, both graders independently delineated the boundaries of the preserved EZ area measured from the en face EZ maps. The delineation did not include the pseudopodial extensions because they were not considered as intact EZ but outer retinal tubulations.¹⁵ B-scans from the same location were reviewed to evaluate the presence of outer retinal tubulations when graders suspected some areas on the EZ map resembled the pseudopodial extensions. The center of the macula was mapped on the EZ map by incorporating the information from B-scans. The horizontal and vertical axes across the macula were also marked. The figures with annotations were then exported from HEYEX2 in TIFF format and imported into Photoshop CC (version 19.1.5) for further analysis. The 45° and 135° reference axes were then added to the figures in Photoshop CC. EZ lengths at 0°, 45°, 90°, and 135° from the same eye were measured by grader 2 using the method we described in our previous publication,¹⁶ and recorded as L_0° , L_{45° , L_{90° , and L_{135° .

Data Analysis for EZ Area and EZ Length

We first compared the EZ area reported by two graders using the intraclass correlation coefficient (ICC). The degree of intergrader agreement was assessed according to the descriptive method of Bland and Altman.¹⁷ For each eye, the absolute difference between two EZ areas measured by two graders was calculated. A mean absolute difference was then generated by taking an average of all the absolute differences from all the study eyes.

In terms of EZ length, we calculated the average of the EZ length at 0° and 90° and recorded it as L_1 ($L_1 = \frac{L_0^\circ + L_{90^\circ}}{2}$). We also calculated the average EZ length at four meridians and recorded that as L_2 ($L_2 = \frac{L_0^\circ + L_{45^\circ} + L_{90^\circ} + L_{135^\circ}}{4}$). We then calculated the correlation (r) between the EZ area and three EZ lengths (L_0° , L_1 , and L_2) using the Pearson correlation coefficient. We also calculated the weighted correlation coefficient (r_{BA}) using the method described by Bland and Altman as a comparison.¹⁸ We plotted the squares of three lengths with the area using general estimating equations to graphically show the correlation between the three EZ lengths with the EZ area. Fisher’s Z trans-

formation was used to calculate Z scores and to test the significance of the difference between two correlation coefficients. Statistical analyses of the data were performed using IBM SPSS software (version 26.0; IBM Corp. Armonk, NY) and STATA (version 14; StataCorp LLC, College Station, TX). The data was plotted by GraphPad Prism (version 8 for Windows 64-bit, San Diego, CA) and Microsoft Excel (Office for Mac, version 16.37, Redmond, WA). The results are presented as mean (standard deviation) in this article.

Qualitative and Quantitative Comparison Between En Face EZ and Preserved FAF

Short-wavelength FAF images were all acquired by using the Heidelberg Spectralis system (Heidelberg Engineering). The acquisition mode was high-speed and the automatic real time setting was greater than 15 frames. All the FAF images cover a retinal field of 30° × 30° area, centered on the fovea. Using the draw region tool of the Heidelberg Eye Explorer 2 (HEYEX2, Heidelberg Engineering, version 1.10.0.0), we measured the preserved FAF area. We compared the preserved FAF measurement with the preserved EZ area, both measured by grader 2, using the Bland–Altman plot.

We also manually aligned the en face EZ map and FAF images by using two fixed reference points (e.g., the branch points of vessels). The alignment was done by using Photoshop CC. Microperimetry data collected by the MAIA microperimeter (Macular Integrity Assessment; CenterVue, Padova, Italy) using a 10-2 (68 stimuli) grid after 30 minutes of dark adaptation was also included for qualitative comparison in the Discussion part of this article. The test points that have significant retinal function (>0 dB) were included in the analysis.

Results

The Generation of the EZ Map

More than 150 imaging records were reviewed from patients with CHM seen in our clinic during in 2014 through 2019. Twenty eyes from 12 male patients with CHM met the inclusion criteria and were included in this study for further analysis. The mean age of this group of patients with CHM was 36.38 (standard deviation, 11.26 years; range, 28–66 years). The visual acuity was recorded as the Early Treatment Diabetic Retinopathy Study letter score. The

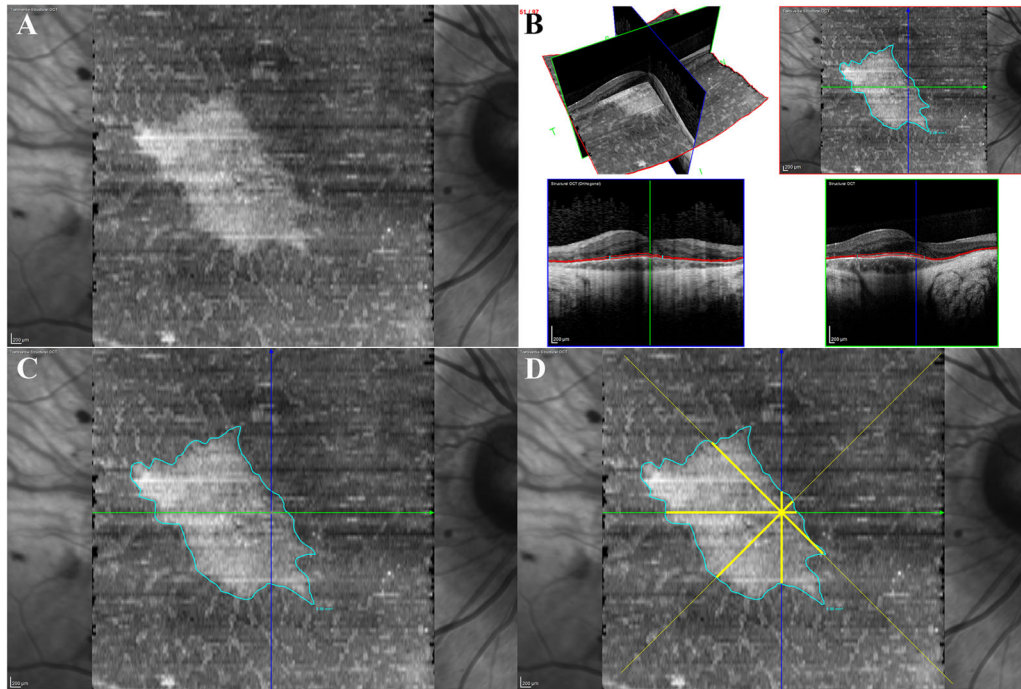


Figure 2. An example of generated en face EZ map (A). The center of macular was mapped by incorporating the information from B-scans (B). The EZ area was measured by using the “draw region” function in HEYEX2 (C). EZ lengths at 0, 45, 90, and 135 were measured by a Photoshop protocol (D).

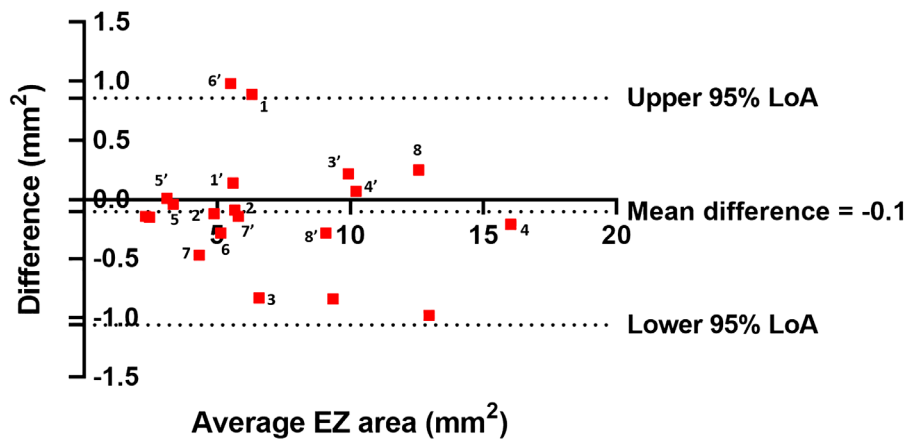


Figure 3. A Bland-Altman plot of preserved EZ area measured by two graders (SO, YZ). The mean difference was 0.1 (0.49) mm². Top and bottom dashed lines: upper and lower 95% limit of agreement (-1.06, 0.86). The eight subjects ($n = 1-8$) with both eyes included in this study are labeled. The measurements from right eyes are labeled as n and the measurements from left eyes are labeled as n' .

mean Early Treatment Diabetic Retinopathy Study letter score for the study eyes was 77.25 (standard deviation, 8.50; range, 52–88). Imaging records were excluded on the basis of poor image quality, improper scan settings. EZ maps for individual eyes were generated and measured successfully (Figs. 2A, B).

EZ Area Measurement by Two Graders

The mean (standard deviation) preserved EZ area measured by grader 1 and grader 2 was 7.01 (3.65) mm² and 7.11 (3.73) mm², respectively. The mean absolute difference between two graders was 0.36 (0.33) mm².

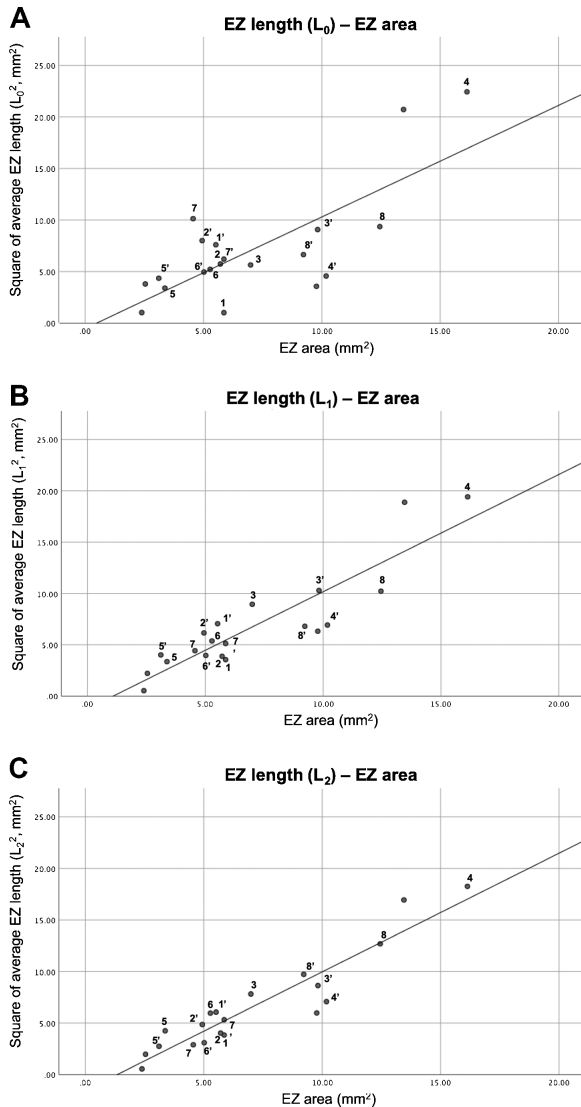


Figure 4. A scatter plot of the EZ lengths and the EZ area. **(A)** the horizontal EZ length has a good correlation with the EZ area with an r_1 of 0.722. **(B)** The average EZ length at 0° and 90° has a better correlation with the EZ area with an r_2 of 0.897. **(C)** The average EZ length in four meridians shows the best correlation with the EZ area with an r_3 of 0.929. The eight subjects ($n = 1$ – 8) with both eyes included in this study are labeled. The measurements from right eyes are labeled as n and the measurements from left eyes are labeled as n' .

The EZ area measured by two graders showed excellent agreement with an ICC of 0.992 (95% confidence interval [CI], 0.980–0.997), where values from 0 to 1 indicate no agreement and 1 indicates perfect agreement.¹⁹ ICC values of less than 0.50, between 0.50 and 0.75, between 0.75 and 0.90, and greater than 0.90 are indicative of poor, moderate, good, and excellent reliability, respectively.²⁰

A Bland–Altman plot comparing the average EZ area of 20 measured pairs, with the difference in measurements between the graders is shown in [Figure 3](#)

and Supplementary Figure S1. The mean bias between graders was 0.10 (0.49) mm^2 , indicating that the results measured by two graders agreed with each other in general. The limit of agreement ranged from -1.06 to 0.86.

Correlation Between EZ Area and EZ Length

The Pearson correlation coefficient (r_1) between horizontal EZ width (L_0) and EZ area was 0.722 (95% CI, 0.410–0.882; $Z = 0.912$; $P < 0.00$). The average EZ length at 0° and 90° (L_1) showed a greater correlation with the EZ area with a r_2 of 0.897 (95% CI, 0.753–0.959; $Z = 1.457$; $P < 0.00$). The average EZ length at four meridians (L_2) showed the greatest correlation with EZ area, with an r_3 of 0.929 (95% CI, 0.826–0.972; $Z = 1.651$; $P < 0.000$). There was a significant difference between r_1 and r_3 ($P = 0.016$), meaning that the L_2 had a significantly better correlation with EZ area compared to the L_0 . Using a weighted correlation coefficient (r_{BA}), we found that L_0 correlated with EZ area ($r_{BA1} = 0.698$; $Z = 0.863$; $P = 0.012$). L_1 had a better correlation with the EZ area with a r_{BA2} of 0.858 ($Z = 1.286$; $P < 0.00$). L_2 showed the greatest correlation with EZ area with a r_{BA3} of 0.904 ($Z = 1.494$; $P < 0.000$). However, owing to a decrease in sample size for this calculation (from 20 to 12), no significant difference between r_{BA1} and r_{BA3} ($P = 0.091$) was observed.

We also plotted the square of the three EZ lengths (L_0 , L_1 , and L_2) with the EZ area and using general estimating equations to show the linear correlation between the length and area ([Fig. 4](#)). This figure suggests that among three groups of EZ lengths, the average EZ length at the four meridians showed the greatest positive correlation with the EZ area. We labeled the eight subjects in whom both eyes were included in this study.

The Comparison Between EZ and FAF

The mean preserved FAF area was measured as 7.55 (4.32) mm^2 . The mean absolute difference between preserved EZ and FAF area was 0.74 (0.77) mm^2 . This difference indicated that two types of quantification methods for retinal structure were not interchangeable. A Bland–Altman plot comparing the differences between FAF area and EZ area of 20 measured pairs is shown in [Figure 5](#) and Supplementary Figure S2. The mean bias between the two mean measurements was 0.45 (0.99) mm^2 , indicating that the FAF area was in general 0.45 mm^2 greater than the EZ area. The limit of agreement ranged from -1.50 to 2.39.

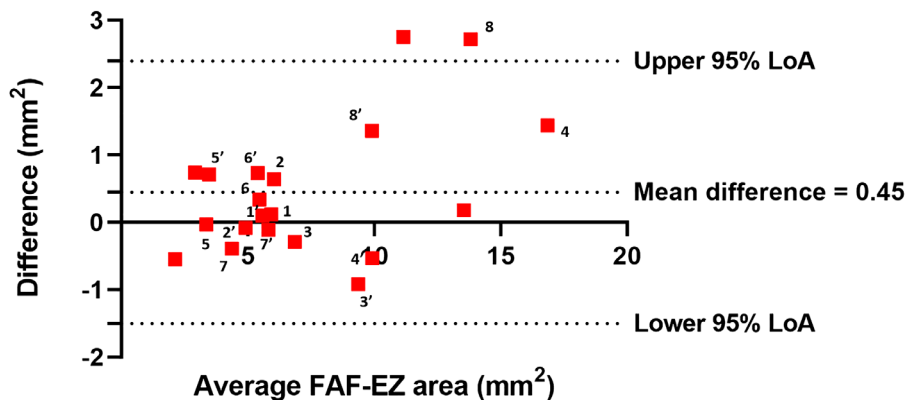


Figure 5. A Bland-Altman plot of preserved FAF area and preserved EZ area (FAF-EZ). The mean difference was 0.45 (0.99) mm². Top and bottom dashed lines: upper and lower 95% limit of agreement (−1.50, 2.39). The eight subjects ($n = 1-8$) with both eyes included in this study are labeled. The measurements from right eyes are labeled as n and the measurements from left eyes are labeled as n'.

Discussion

EZ as an Outcome Measurement for Ocular Gene Therapy Trials

By consensus, the EZ is referred to as the second hyper-reflective band on SD-OCT and has been anatomically correlated with the photoreceptor inner segment.²¹ EZ disruption or EZ loss has been used as a measure of disease severity in some retinal diseases, such as geographic atrophy²² and Stargardt disease.²³ CHM, in contrast, has a different clinical course compared with these retinal diseases. The characteristic lesion of CHM is chorioretinal scalloped atrophy in the midperipheral fundus, with preservation of the macula.²⁴ Thus, an accurate measure of preserved EZ area has the potential to be used as a marker to monitor disease progression as well as to evaluate the efficacy of experimental therapies. Hariri et al²⁵ estimated the preserved EZ area in patients with CHM by using the EZ band lengths from each B-scan and had some success. However, their method did not provide an en face EZ map for further studies on the correlation between the EZ and other imaging data. The EZ maps we created in this study maintain important landmarks that can be used as fixed reference points (e.g., the branch points of vessels). Thus, we are able to use en face EZ maps to conduct multimodal structure–function analysis.

In the present study, we assessed a new method to generate an en face EZ map from the OCT volume scan of patients with CHM. The EZ area measurements by two graders showed excellent agreement with an ICC of 0.992 (95% CI, 0.980–0.997), indicating that it could be used in future clinical trials as an accurate

way to quantify photoreceptor structure. However, we must admit that the segmentation process for measuring the EZ area was very time consuming. Two graders each worked for 8 hours to finish a precise segmentation for EZ area from a single OCT volume scan. As such, developing an automatic algorithm to create the en face EZ map would be a preferred approach in the future. Wang et al²⁶ developed a method to automatically detect photoreceptor structure in CHM using machine learning with some success; however, their results still showed a significant disagreement between manual segmentation and automated segmentation, which would be unsuitable for applications in clinical trials. This result makes manual segmentation, as undertaken in this study, the only suitable approach because it is currently the only precise way to map the preserved EZ area.

EZ band length from B-scan was used as a marker to trace photoreceptor changes in X-linked retinitis pigmentosa.¹² Our laboratory measured the EZ across the macula as a marker for photoreceptor structure in our previous CHM gene therapy trial.⁴ However, the preserved EZ area in CHM is typically irregular; therefore, using the horizontal preserved EZ band length may not accurately measure the preserved photoreceptors. Our data suggest a combination of the EZ length in four meridians across the macula may improve the estimate of the preserved photoreceptor area. A high-resolution line scan in four meridians across the macula may be a good OCT testing mode to the estimate EZ area, which could be a powerful tool for future CHM gene therapy trials.

We also studied the interocular correlation of EZ area and EZ length in the subjects in whom both eyes were included. We found significant interocular correlation in EZ area ($r = 0.821$; $P = 0.012$)

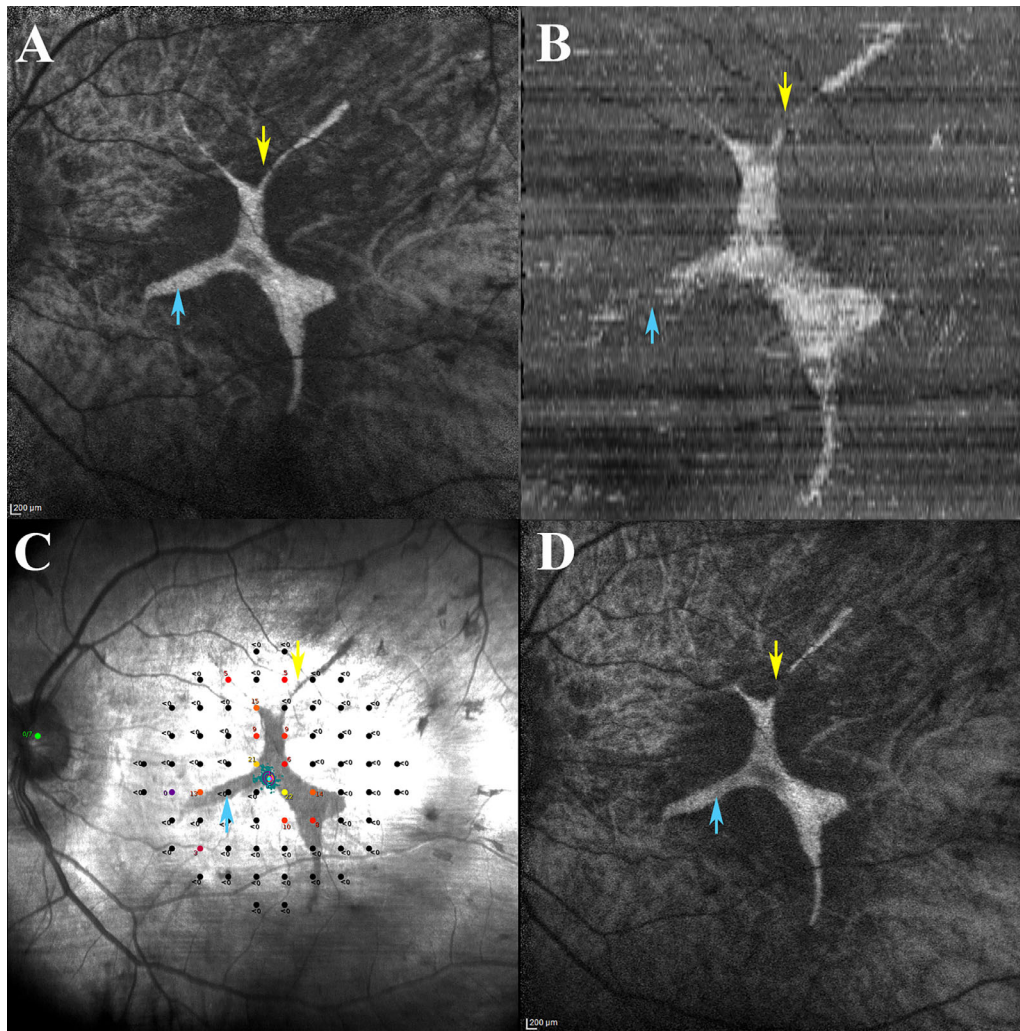


Figure 6. An example of the difference between FAF and EZ. The FAF image (A) and the en face EZ map (B) were both obtained at the same visit. The areas that lacked EZ but had FAF preservation are marked with arrows. Microperimetry data from the same visit (C) shows that both areas lack significant visual function. Another FAF image (D) taken 4 years after (A) suggests that the areas that lack EZ but have FAF preservation either have totally lost FAF signal (yellow arrows) or have great decrease in FAF signal intensity (blue arrows).

(Supplementary Fig. S3). However, there was no significant interocular correlation in horizontal EZ length ($r = -0.357$; $P = 0.386$) and average EZ length in four meridians ($r = 0.579$; $P = 0.132$) (Supplementary Figs. S4 and S5).

Correlation Between EZ and FAF

Based on our comparison between the EZ and FAF area (Fig. 5), we found that the preserved FAF area is generally larger than the preserved EZ area. One example of this difference is shown in Figure 6. According to the FAF (Fig. 6A) and en face EZ images (Fig. 6B) obtained at the same visit, the FAF area was measured as 3.82 mm^2 and the EZ area was measured as 3.11 mm^2 . The areas that created this difference are

marked with arrows (Fig. 6). Microperimetry data from the same visit also suggested that these areas did not have a significant visual function (arrows, Fig. 6C). By observing the FAF image 4 years after the baseline (Fig. 6D), we noticed that the areas that lacked the EZ but had FAF preservation (arrows) either had a total loss of FAF signal (yellow arrows) or had a great decrease in FAF signal intensity (blue arrows). A possible explanation would be that the impairment of photoreceptor inner segment structure occurs before the total destruction of the RPE cells. A lack of EZ may be the earliest observation in the natural history of CHM. This observation indicates that we should pay more attention to these areas in a CHM clinical trial, because the retinal function in these area is more likely to be reversible.

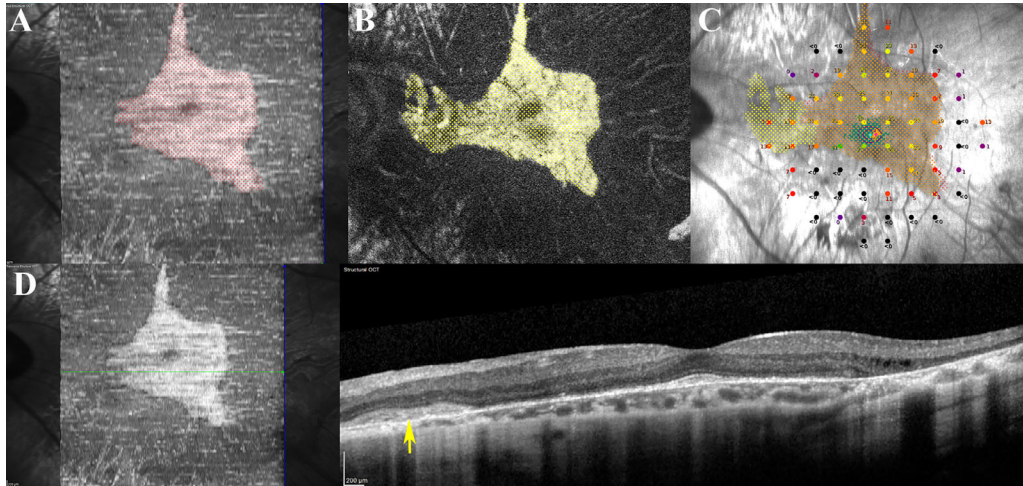


Figure 7. The projection of preserved EZ area (pink, **A**) and preserved FAF (yellow, **B**) on the microperimetry (**C**). The overlap of the EZ and FAF is shown as orange in the microperimetry (**C**), and has good retinal sensitivity (5–31 dB). The preserved FAF lacking EZ is marked with yellow (**C**) still has some preserved retinal sensitivity (7–17 dB). OCT scan across the yellow area in **C** (**D**) shows a peripapillary choroidal neovascular membrane (CNVM, yellow arrow) with some preservation of FAF but a total loss of the EZ.

When reviewing and comparing the EZ map and FAF images manually, we noticed some eyes with the greatest difference between preserved EZ and FAF area had another underlying pathologic condition. One case had a rare peripapillary choroidal neovascular membrane, resulting in a disagreement in the EZ and FAF area. The areas within or close to the neovascular membrane lack an EZ but have some preservation of FAF signal. To understand this difference between the en face EZ and the FAF distribution better, we aligned the en face EZ map, FAF as well as microperimetry from this eye (Fig. 7). We found the area that had both preserved FAF and EZ (orange area in Fig. 7C) had an average sensitivity of 20.2 dB. The area that lacked the EZ but had FAF preservation (yellow area in Fig. 7C) had an average sensitivity of 13.0 dB. Some points outside the preserved FAF area tested as functional in microperimetry; the average sensitivity for these points was 6.2 dB. These findings suggested that the disruption of the photoreceptor inner segment ellipsoid may be an early structural change in the choroidal neovascular membrane, which happens before the disruption of RPE. This change is directly correlated with a decreased retinal function. This observation is another piece of evidence to show that a combination of en face EZ mapping with other imaging modalities can be a helpful approach for us to learn the pathologic process in CHM.

Our study has some limitations. For example, we used plain Bland–Altman plots to present the agreement between the two graders. Because we have eight

study subjects who had both eyes included in this study, a modified method to measure agreement for repeated measurements may be more appropriate. However, because we do not have access to such a statistical function, we only reported plain Bland–Altman plots and limits of agreement here. According to Bland and Altman, the estimate of bias will be unaffected by the averaging, but the estimate of the standard deviation of the differences will be relatively smaller.²⁷ Second, because CHM is a rare disease and we used strict inclusion criteria, the study sample size was still limited.

In summary, we used a novel method to create an en face EZ map, and to quantify preserved EZ areas in CHM. This method provides excellent intergrader reliability, although the process is time consuming. We also provide an alternative way to estimate EZ area using the average EZ band length in meridians. Our data suggest that a loss of the photoreceptor inner segment seems to be an early change in the CHM, which happens before the loss of RPE.

Acknowledgments

The authors thank Manlong Xu (University of Alberta) and Ioannis Dimopoulos (University of Ottawa) for their efforts on acquiring the high quality images. The authors thank Milo Shaoqing Wang

(University of Alberta) for his insights on the statistical analysis and Kimberly Papp (University of Alberta) for her comments on this article.

Supported by Choroideremia Research Foundation and Choroideremia Research Foundation Canada.

Disclosure: **Y. Zhai**, None; **S. Oke**, None; **I.M. MacDonald**, None

References

1. Cremers FP, Sankila EM, Brunsmann F, et al. Deletions in patients with classical choroideremia vary in size from 45 kb to several megabases. *Am J Hum Genet.* 1990;47:622–628.
2. Kalatzis V, Hamel CP, MacDonald IM. First international choroideremia research symposium. Choroideremia: towards a therapy. *Am J Ophthalmol.* 2013;156:433–437.e433.
3. MacLaren RE, Groppe M, Barnard AR, et al. Retinal gene therapy in patients with choroideremia: initial findings from a phase 1/2 clinical trial. *Lancet.* 2014;383:1129–1137.
4. Dimopoulos IS, Hoang SC, Radziwon A, et al. Two-year results after AAV2-mediated gene therapy for choroideremia: the Alberta experience. *Am J Ophthalmol.* 2018;193:130–142.
5. Lam BL, Davis JL, Gregori NZ, et al. Choroideremia gene therapy phase 2 clinical trial: 24-month results. *Am J Ophthalmol.* 2019;197:65–73.
6. Fischer MD, Ochakovski GA, Beier B, et al. Efficacy and safety of retinal gene therapy using adeno-associated virus vector for patients with choroideremia: a randomized clinical trial. *JAMA Ophthalmol.* 2019 ;137:1247–1254.
7. Spaide RF, Curcio CA. Anatomical correlates to the bands seen in the outer retina by optical coherence tomography: literature review and model. *Retina.* 2011;31:1609–1619.
8. Khan KN, Islam F, Moore AT, Michaelides M. Clinical and genetic features of choroideremia in childhood. *Ophthalmology.* 2016;123:2158–2165.
9. Heon E, Alabduljalil T, McGuigan ID, et al. Visual function and central retinal structure in choroideremia. *Invest Ophthalmol Vis Sci.* 2016;57:OCT377–OCT387.
10. Hagag AM, Mitsios A, Narayan A, et al. Prospective deep phenotyping of choroideremia patients using multimodal structure-function approaches. *Eye. (Lond)* 2020;35:838–852.
11. Tao LW, Wu Z, Guymer RH, Luu CD. Ellipsoid zone on optical coherence tomography: a review. *Clin Exp Ophthalmol.* 2016;44:422–430.
12. Birch DG, Locke KG, Wen Y, Locke KI, Hoffman DR, Hood DC. Spectral-domain optical coherence tomography measures of outer segment layer progression in patients with X-linked retinitis pigmentosa. *JAMA Ophthalmol.* 2013;131:1143–1150.
13. Murro V, Mucciolo DP, Sodi A, et al. En face OCT in choroideremia. *Ophthalmic Genet.* 2019;40:514–520.
14. Hariri AH, Zhang HY, Ho A, et al. Quantification of ellipsoid zone changes in retinitis pigmentosa using en face Spectral Domain-optical coherence tomography. *JAMA Ophthalmol.* 2016;134:628–635.
15. Dolz-Marco R, Litts KM, Tan ACS, Freund KB, Curcio CA. The evolution of outer retinal tubulation, a neurodegeneration and gliosis prominent in macular diseases. *Ophthalmology.* 2017;124:1353–1367.
16. Zhai Y, Xu M, Dimopoulos IS, et al. Quantification of RPE changes in choroideremia using a Photoshop-based method. *Transl Vis Sci Technol.* 2020;9:21.
17. Bland JM, Altman DG. Statistical methods for assessing agreement between two methods of clinical measurement. *Lancet.* 1986;1:307–310.
18. Bland JM, Altman DG. Calculating correlation coefficients with repeated observations: part 2—Correlation between subjects. *BMJ.* 1995;310:633.
19. Ranganathan P, Pramesh CS, Aggarwal R. Common pitfalls in statistical analysis: measures of agreement. *Perspect Clin Res.* 2017;8:187–191.
20. Koo TK, Li MY. A guideline of selecting and reporting intraclass correlation coefficients for reliability research. *J Chiropr Med.* 2016;15:155–163.
21. Staurengi G, Sadda S, Chakravarthy U, Spaide RF, International Nomenclature for Optical Coherence Tomography Panel. Proposed lexicon for anatomic landmarks in normal posterior segment spectral-domain optical coherence tomography: the IN*OCT consensus. *Ophthalmology.* 2014;121:1572–1578.
22. Giocanti-Auregan A, Tadayoni R, Fajnkuchen F, Dourmad P, Magazzeni S, Cohen SY. Predictive value of outer retina en face OCT imaging for geographic atrophy progression. *Invest Ophthalmol Vis Sci.* 2015;56:8325–8330.
23. Cai CX, Light JG, Handa JT. Quantifying the rate of ellipsoid zone loss in Stargardt disease. *Am J Ophthalmol.* 2018;186:1–9.

24. Lee TK, McTaggart KE, Sieving PA, et al. Clinical diagnoses that overlap with choroideremia. *Can J Ophthalmol*. 2003;38:364–372; quiz 372.
25. Hariri AH, Velaga SB, Girach A, et al. Measurement and reproducibility of preserved ellipsoid zone area and preserved retinal pigment epithelium area in eyes with choroideremia. *Am J Ophthalmol*. 2017;179:110–117.
26. Wang Z, Camino A, Hagag AM, et al. Automated detection of preserved photoreceptor on optical coherence tomography in choroideremia based on machine learning. *J Biophotonics*. 2018;11:e201700313.
27. Bland JM, Altman DG. Measuring agreement in method comparison studies. *Stat Methods Med Res*. 1999;8:135–160.